

DR KE MA (Orcid ID : 0000-0002-6538-1137)

Article type : Article

## Low-temperature synthesis of tungsten diboride powders via a simple molten salt route

Ke Ma, Xiangxin Xue, Xiaozhou Cao

Liaoning Key Laboratory of Metallurgical Resources Recycling Science, Northeastern University, Shenyang 110819, China

### Correspondence

Xiangxin Xue, Liaoning Key Laboratory of Metallurgical Resources Recycling Science, Northeastern University, Shenyang 110819, China  
Email: Xuexx@mail.neu.edu.cn

### Abstract

WB<sub>2</sub> powders were successfully prepared at 1000°C using NaCl-KCl salts as molten salts. Compared to the conventional solid-state reaction, the introduction of NaCl-KCl salts decreased the synthesis temperature of WB<sub>2</sub> phase, which was related to the faster diffusion rate of particles in the liquid state than in the solid-state. The effect of reaction temperature, time and the amount of molten salts on the synthesis of WB<sub>2</sub> were studied in detail. The template formation mechanism was considered to have played an essential part in the synthesis process. TEM analysis showed that the as-synthesized WB<sub>2</sub> powders exhibited a hexagonal crystal structure. Furthermore, the oxidation protective performance of as-synthesized WB<sub>2</sub> powders was investigated by TG-DSC. This article has been accepted for publication and undergone full peer review but has not been through the copyediting, typesetting, pagination and proofreading process, which may lead to differences between this version and the [Version of Record](#). Please cite this article as [doi: 10.1111/IJAC.13427](https://doi.org/10.1111/IJAC.13427)

This article is protected by copyright. All rights reserved

measurement.

## KEYWORDS

WB<sub>2</sub>, molten salt synthesis, template formation mechanism, oxidation resistance

## 1 | INTRODUCTION

Nowadays, high-temperature ceramics including transition metal borides, nitrides, and carbides are expected to be used in aerospace and other applications [1, 2]. Among the existing ceramics materials, tungsten borides have the characteristic of high hardness, high melt point, chemical inertness, and excellent chemical stability, which have good prospects for application in high temperature structural, wear-resistant hard-wearing, corrosion-resistant and electrode materials [3-7]. Therefore, it is essential to develop the experimental research of tungsten borides. Based on the existing literature, different borides such as W<sub>2</sub>B, WB, W<sub>2</sub>B<sub>5</sub>, WB<sub>2</sub>, WB<sub>4</sub>, and WB<sub>12</sub> were reported in the W-B system [8-12]. However, previous studies focus intensively on the theoretical prediction [13-15]. So there is still a lot of experimental work to do.

WB<sub>2</sub> was originally prepared in 1966 [16]. Summarizing literature, tungsten diboride has been synthesized by solid-state reaction, chemical vapor deposition, molten salt electrolysis, floating zone method, and self-propagating high-temperature synthesis [14-17]. These techniques suffered from several disadvantages: relatively high reaction temperature, complicated process, and agglomerated and impure product. These problems would be correctly solved by the molten salt synthesis (MSS) route, which can provide a liquid phase environment for the reaction process [21-23]. The thoroughly blending of the raw materials at the molecular or atomic level is achieved, and the energy required for the reaction is greatly reduced from the kinetics. As a result, the diffusion speeds of reactants can be accelerated and the synthesis temperature can be greatly lowered [24, 25]. So products generally possess a good crystallinity and crystalline morphology.

In the present work, WB<sub>2</sub> was prepared by the molten salt synthesis method using W and amorphous B as starting materials. NaCl-KCl salts were introduced to provide a liquid environment. The effects of reaction temperature, reaction time and reactants/salts weight ratio on

the synthesis process of WB<sub>2</sub> powders were studied in detail. The oxidation resistance of WB<sub>2</sub> powders was also analyzed in this paper. Through the study, it aimed to lay the foundation of further studying in the preparation and properties of ceramics.

## 2 | EXPERIMENTAL PROCEDURE

Amorphous boron powders (B, purity of 95%, 3 μm, Dandong ), tungsten powders (W, purity of 99.9%, 1μm, Shanghai ) were used as starting materials. Salts including NaCl and KCl (purity of 99.5%, Sinopharm Chemical Reagent Co., Ltd) were used to provide a molten salts medium. As is known that NaCl and KCl have melting points of 801°C and 771°C, respectively. While eutectic salts of NaCl and KCl provide a lower melting point of 657°C with a molar ratio of 1:1. The reactant W/B molar ratio was 1:2. And the reactants/salts weight ratio was set as 1:3, 1:6 and 1:10, respectively. The reactant and salts were then mixed by hand for 0.5 h with an agate mortar. The powders mixture was put into an alumina crucible with a lid. The crucible with the powders mixture was placed in an alumina tube furnace for heating treatment. The heating and cooling process was protected by flowing argon. The tube furnace was heated to 800°C, 900°C, 1000°C, 1100°C, and 1200°C respectively, with a heating rate of 10°C/min, and held for 3 h. After cooling to room temperature, the as-obtained products in the alumina crucible was taken out and repeatedly washed with boiled deionized water, and then filtered to remove the salts completely. Finally, the products were dried at 80°C for further characterization.

The phase composition of as-synthesized powders was measured by X-ray diffraction (XRD, PANalytical, NETHERLANDS) using Cu Ka radiation. The morphology and microstructure of as-prepared powders were analyzed by a transmission electron microscope (TEM, JEM-2100, JAPAN). To evaluated the oxidation resistance property and understand the oxidation behavior of WB<sub>2</sub>, TG-DSC analysis was performed in air ranging from 0°C to 1000°C at a rate of 10°C/min.

## 3 | RESULTS AND DISCUSSION

### 3.1 | Effect of heating temperature on the synthesis of WB<sub>2</sub> powders

Figure 1 shows the XRD patterns of powders synthesized at various temperatures for 3 h with the reactants/salts weight ratio of 1:3. As the temperature was 800°C, the poor crystallized WB phase (PDF no. 01-073-1769) appears, indicating that the W phase firstly reacts with B to form WB phase. Here, WB<sub>2</sub> phase was not found in the XRD pattern, which indicates that the formation of WB<sub>2</sub> must be above 800°C. When the temperature increased to 900°C, WB<sub>2</sub> phase (PDF no. 00-043-1386) was produced along with WB phase. The diffraction peaks (004) (100) (101) (105) (110) and (114) of WB<sub>2</sub> can be observed in the XRD pattern, indicating that WB reacts with unreacted B to form WB<sub>2</sub>. At 1000°C for 3h, WB phase disappeared entirely, and only WB<sub>2</sub> phase was detected in the XRD pattern. Compared to the solid-solid reaction, the MSS method could provide a liquid environment that was helpful to increase the degree of homogeneity and the diffusion rate. Thus, it decreased the energy required for the reactions from dynamics. Upon increasing the temperature to 1200°C, the peaks (1 0 3) (1 0 5) and (1 1 2) of WB phase occurred. There are volatilization loss of molten salts at higher temperature (>1200°C), which decreased the diffusion and reaction rate and resulted in the incomplete reaction. As a result, unreacted WB phase can also be seen from the XRD patterns. When the B/W molar ratio increased to 2.5, no trace of WB was detected, and pure WB<sub>2</sub> was obtained as the only phase, indicating the existence of excess B contributes to the completion of the reactions.

### 3.2 | Effect of reaction time on the synthesis of WB<sub>2</sub> powders

The effect of the reaction time of 1, 2 and 3 h on the phase analysis of the powder with B/W molar ratio of 2 and reaction temperature of 1000°C are shown in Figure 2. At 1000°C, the formation of WB<sub>2</sub> is evident regardless of reaction time. For powder prepared for 1 and 2 h, the dominant phase was WB<sub>2</sub> and slight peaks of WB were observed. By increasing reaction time from 1 h to 3 h, the intensity of WB<sub>2</sub> peaks increased and the peaks of WB disappeared totally. Longer time would cause grain coarsening. To sum up, the optimum reaction time is 3 h for the synthesis of WB<sub>2</sub>, because the synthesis process is complete and the products are single-phase.

### 3.3 | Effect of the amount of NaCl-KCl salts on the synthesis of WB<sub>2</sub> powders

Figure 3 shows the effect of the reactants/salts weight ratio on the phase composition of the samples synthesized at 1000°C with B/W molar ratio of 2. Without the addition of NaCl-KCl salts, only W phase could be detected in the XRD patterns and no reactions occurred, which showed the diffusion rate and reaction rate was extremely low at 1000°C without molten salts. It can be seen that the as-synthesized products consisted of a dominant WB<sub>2</sub> phase with the addition of NaCl-KCl salts. Besides, a minor WB phase was also found in the products especially when the reactants/salts weight ratio was 1:9. It can be explained that excess molten salts made it difficult for the reactants to contact each other, which slowed down the reaction process. Furthermore, the interstices of the reactant particles can't contain all the molten salt, resulting in a large amount of the molten salt seeping out of the reactants. Seeped molten salt never acts as a solvent. Figure 4 shows the SEM micrographs of the products synthesized at 1000°C for 3 h with different reactants/salts weight ratio. It can be seen that there was no noticeable difference in the shapes and sizes of the products as the reactants/salts weight ratio increased. It's worth noting that the size of particles was in the range of 0.5~2.5 μm. The particles seem not so small, and this has something to do with the template formation mechanism, which would be discussed in the following part.

### 3.4 | Crystal structure of WB<sub>2</sub>

WB<sub>2</sub> has a hexagonal crystal structure (space group P6<sub>3</sub>/mmc;  $a=2.9831\text{ \AA}$  and  $c=13.879\text{ \AA}$ ) [26] as shown in Figure 5C. It can be seen that W atoms are close to the planar hexagonal B-layers and puckered B-layers with short B-B distances of 1.722(1) Å and 1.850 Å, respectively. It is evident that the excellent mechanical properties but poor sinterability of WB<sub>2</sub> are caused by its strong B-B covalent bonding.

TEM analysis was performed to confirm further the as-synthesized powder was WB<sub>2</sub>. As shown in the inserted image in Figure 5B, the SAED pattern corroborates that the WB<sub>2</sub> particle was highly crystallized. The pattern along [0 0 1] zone axis verified the characterized particle was WB<sub>2</sub>.

### 3.5 | Molten salts synthesis mechanism

---

NaCl-KCl salts melt at 657°C, providing a liquid environment for the formation process of the WB<sub>2</sub> phase. It is noteworthy that reactants tungsten powders and amorphous boron are in the form of solid-state in the molten salts. There are two possible mechanisms involved in the molten salt synthesis process according to the solubilities of the reactants: “dissolution-precipitation” mechanism and “template formation” mechanism. As a result, the solubility of the reactants in the molten salts plays an important part in the synthesis of WB<sub>2</sub> powders and the morphology of the final product. However, the data about the solubility of B and W in molten salts are unavailable. So we try to explain the mechanism of the formation process of WB<sub>2</sub> phase according to the morphology of final powders as shown in SEM photos. So far, two accepted mechanisms were usually used to explain the molten salt synthesis process, including the template formation mechanism and the dissolution-precipitation mechanism. If the formation process of WB<sub>2</sub> phase was mainly controlled by the dissolution-precipitation mechanism, the final powder particle should be spherical, which is not consistent with the near hexagonal shape of WB<sub>2</sub> particles observed in the SEM image (Figure 5A). As a result, this mechanism for explaining the formation of WB<sub>2</sub> powders was ruled out. But for template formation mechanism, if one reactant is more soluble in molten salt than the other, the more soluble reactant would diffuse into the surface of the less soluble one and react to form the product. As a result, the obtained powders usually retain the size and similar morphology of the raw reactant (less soluble) [27]. To sum up, the template formation mechanism may play a dominant role in the MSS process.

Based on the presented results and above discussion, a plausible mechanism for the whole MSS process to form the WB<sub>2</sub> phase can be schematically illustrated in Figure 6. First, when the temperature increased to 658°C, NaCl-KCl salts begin to melt. If the temperature continued to rise, the salts melted entirely and provided a liquid environment for the following reactions. So the raw reactants can be mixed homogeneously in molten salts at the atomic level. As a consequence, as the temperature increased to 800°C, amorphous boron powders would diffuse into the surface of tungsten powders to synthesize WB powders according to the XRD results. When the heating temperature up to 1000°C, excess boron powders moved into the surface of the synthesized WB

and started to generate  $\text{WB}_2$  phase. With the extension of heating time,  $\text{WB}_2$  powders would be the only phase in the molten salts.

### 3.6 | The thermal stability of $\text{WB}_2$

As a promising high-temperature structural material, the thermal stability of  $\text{WB}_2$  material is also a key index. To evaluate the oxidation resistance of  $\text{WB}_2$  powders, the TG-DSC-DTG curves of the sample in the flowing air at temperatures range 0-1000°C were plotted in Figure 7. It seems that the initial oxidation temperature of  $\text{WB}_2$  powders is approximately 400°C, from which the weight gain appears owing to the formation of tungsten oxides and boron oxide. With the increase of the oxidation temperature, the weight gain of the sample becomes faster as shown in the DTG curve, indicating that  $\text{WB}_2$  powders begin to oxidize quickly above this temperature. However, as the temperature increases to 633.82°C, the oxidation rate of the sample is found to be slow. Finally,  $\text{WB}_2$  powders can be oxidized thoroughly at 790°C, and the weight gain remains almost constant on the TG curve when the temperature is between 790°C, and 1000°C, suggesting almost no weight change. It can also be verified from the DSC plot that the oxidation process mainly occurs in the temperature range 400-790°C, at which an evident exothermic peak can be observed.

## 4 | CONCLUSIONS

In this study,  $\text{WB}_2$  powders were successfully synthesized by a molten salts synthesis method. The molten salts provide a liquid environment that enabled the completion of the reaction at a low temperature of 1000°C. The effect of reaction temperature, time, and the amount of molten salts on the  $\text{WB}_2$  formation were studied in detail. It can be seen that the WB phase was first synthesized in the synthesis process and then transformed into  $\text{WB}_2$  phase. It required appropriate reaction time and amount of molten salts to produce pure  $\text{WB}_2$  powders. The template formation mechanism was considered to have played an essential part in the synthesis process. TG-DSC was employed to evaluate the oxidation resistance of as-synthesized  $\text{WB}_2$  powders, showing its good thermal stability.

---

## ACKNOWLEDGMENTS

This study was supported by the National Natural Science Foundation of China (Nos. 51204043, 51472048).

## ORCID

Ke Ma <https://orcid.org/0000-0002-6538-1137>

## References

- [1] Albert B, Hillebrecht H. Boron: Elementary Challenge for Experimenters and Theoreticians. *Angew Chem Int Ed Engl.* 2009;48: 8640-8668.
- [2] Ivan p Parkin. Solid state metathesis reaction for metal borides, silicides, pnictides and chalcogenides: ionic or elemental pathways. *Chem Soc Rev.* 1996;25: 199-207.
- [3] Jiang CL, Pei ZL, Liu YM, Xiao JQ, Sun C. Preparation and characterization of superhard AlB<sub>2</sub>-type WB<sub>2</sub> nanocomposite coatings. *Phys Status Solidi A.* 2013;210: 1221-1227.
- [4] Chong XY, Jiang YH, Zhou R, Feng J. Stability, chemical bonding behavior, elastic properties and lattice thermal conductivity of molybdenum and tungsten borides under hydrostatic pressure. *Ceram Int.* 2016;42: 2117-2132.
- [5] Lv Y, Wen G, Lei TQ. Tribological behavior of W<sub>2</sub>B<sub>5</sub> particulate reinforced carbon matrix composites. *Mater Lett.* 2006;60: 541-545.
- [6] Koval'Chenko MS, Bodrova LG, Nemchenko VF, Kolotun VF. Some physical properties of the higher borides of molybdenum and tungsten. *J Less Common Metals.* 1979;67: 357-362.
- [7] Stadler S, Winarski RP, McLaren JM, Ederer DL, Vanek J, Moewes A, Grush MM, Callcott TA, Perera RCC. Electronic structures of the tungsten borides WB, W<sub>2</sub>B and W<sub>2</sub>B<sub>5</sub>. *J Electron Spectrosc.* 2000;110: 75-86.
- [8] Okada S, Kudou K, Lundström T. Preparations and some properties of W<sub>2</sub>B, δ-WB and WB<sub>2</sub> crystals from high-temperature metal solutions. *Jpn J Appl Phys.* 1995;34: 226-231.
- [9] Itoh H, Matsudaira T, Naka S, Hamamoto H, Obayashi M. Formation process of tungsten borides by solid state reaction between tungsten and amorphous boron. *J Mater Sci.* 1987;22: 2811-2815.

- 
- [10] Cheng XY, Chen XQ, Li DZ, Li YY. Computational materials discovery: the case of the W-B system. *Acta Crystallogr B*. 2014;70: 85-103.
- [11] Duschanek H, Rogl P. Critical assessment and thermodynamic calculation of the binary system boron-tungsten (B-W). *Journal of Phase Equilibria*. 1995;16: 150-161.
- [12] Mohammadi R, Lech AT, Xie M, Weaver BE, Yeung MT, Tolbert SH, Kaner RB. Tungsten tetraboride, an inexpensive superhard material. *P Natl Acad Sci USA*. 2011;108: 10958-10962.
- [13] Zhao CM, Duan YF, Gao J, Liu WJ, Dong HM, Dong HF, Zhang DK, Oganov AR. Unexpected stable phases of tungsten borides. *Phys Chem Chem Phys*. 2018;20: 24665-24670.
- [14] Chen XQ, Fu CL, Krcmar M, Painter GS. Electronic and structural origin of ultraincompressibility of 5d transition-metal diborides  $M\text{B}_2$  ( $M=\text{W}, \text{Re}, \text{Os}$ ). *Phys Rev Lett*. 2008;100: 196403.
- [15] Zhang HY, Xi F, Zeng ZY, Chen XR, Cai LC. First-principles predictions of phase transition and mechanical properties of tungsten diboride under pressure. *J Phys Chem C*. 2017;121: 7397-7403.
- [16] Woods HP, Wawner FE, Fox BG. Tungsten diboride: preparation and structure. *Science*. 1966;151: 75.
- [17] Cao XZ, Xue XX, Yang H, Li HT, Wang HY, Shi LH. Preparation of tungsten boride powder by high-temperature solid-state reaction. *Rare Metal Mat Eng*. 2014;43: 1987-1990.
- [18] Otani S, Ishizawa Y. Preparation of  $\text{WB}_{2-x}$  single crystals by the floating zone method. *J Cryst Growth*. 1995;154: 202-204.
- [19] Yazici S, Derin B. Production of tungsten boride from  $\text{CaWO}_4$  by self-propagating high-temperature synthesis followed by HCl leaching. *Int J Refract Met H*. 2011;29: 90-95.
- [20] Malyshev VV, Kushkhov HB, Shapoval VI. High-temperature electrochemical synthesis of carbides, silicides and borides of VI-group metals in ionic melts. *J Appl Electrochem*. 2002;32: 573-579.
- [21] Liu D, Wen TQ, Ye BL, et al. Molten salt synthesis, characterization, and formation mechanism of superfine  $(\text{Hf}_{x}\text{Zr}_{1-x})\text{B}_2$  solid-solution powders. *J Am Ceram Soc*. 2019;102: 3767-3770.
- [22] Wen TQ, Ning SS, Liu D, et al. Synthesis and characterization of the ternary metal diboride solid-solution nanopowders. *J Am Ceram Soc*. 2019;102: 4956-4962.
- [23] Liu D, Chu YH, Jing SY, et al. Low-temperature synthesis of ultrafine  $\text{TiB}_2$  nanopowders by molten-salt assisted borothermal reduction. *J Am Ceram Soc*. 2018;101: 5299-5303.
- [24] Liu XF, Nina F, Markus A. Salt melt synthesis of ceramics, semiconductors and carbon nanostructures.

Chem Soc Rev. 2013;42: 8237-8265.

- [25] Portehault D, Devi S, Beaunier P, Gervais C, Giordano C, Sanchez C, Antonietti M. A general solution route toward metal boride nanocrystals. *Angew Chem.* 2011;123: 3320-3323.
- [26] Ma K, Cao XZ, Xue XX. Mechanical properties, microstructure and grain orientation of hot pressed  $WB_2$  ceramics with Co as a sintering additive. *Ceram Int.* 2019;45: 14718-14727.
- [27] Yang ZP, Wei LL, Chang YF, Liu B. Synthesis of anisometric  $KSr_2Nb_5O_{15}$  particles in the  $SrNb_2O_6-Nb_2O_5-KCl$  system. *J Mater Sci.* 2007;42: 3627-3631.

### Figure Caption

**FIGURE 1** XRD patterns of powders synthesized at various temperatures for 3 h with a reactants/salts weight ratio of 1:3.

**FIGURE 2** XRD patterns of powders synthesized at 1000°C for different reaction time.

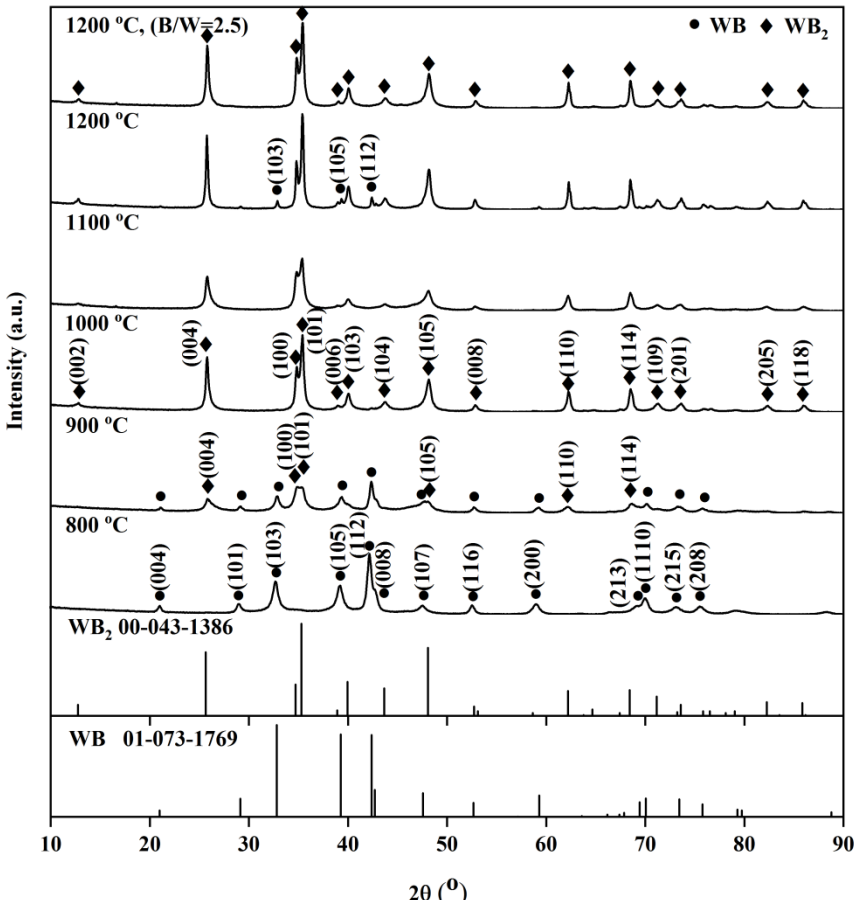
**FIGURE 3** XRD patterns of powders synthesized at 1000°C for 3 h with different reactants/salts weight ratio.

**FIGURE 4** SEM micrographs of the as-synthesized  $WB_2$  powders at 1000°C for 3 h with different reactants/salts weight ratio: (A) 3 time, (B) 6 time, and (C) 9 time.

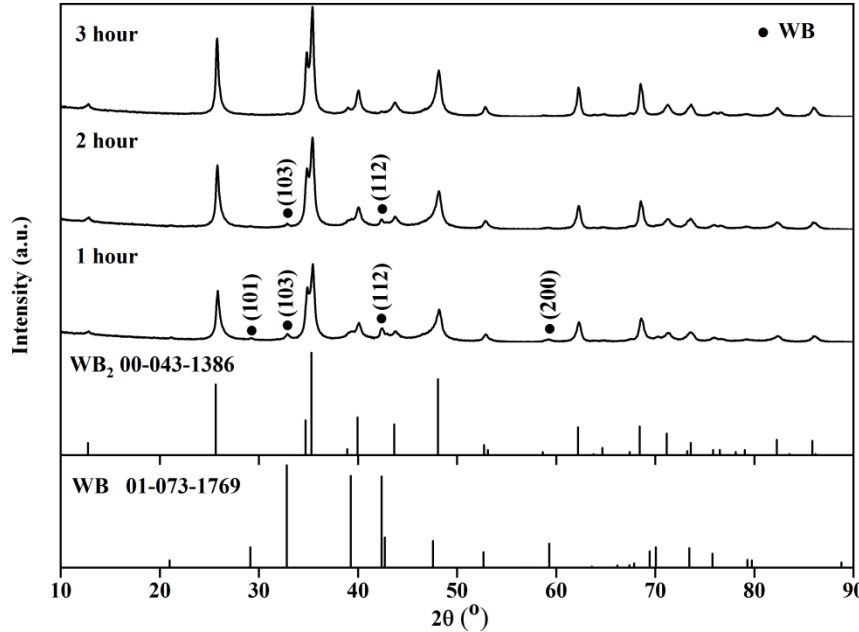
**FIGURE 5** (A) SEM image of the as-synthesized WB<sub>2</sub> powders, (B) TEM image and inserted corresponding selected-area electron diffraction pattern, and (C) The crystal structure of WB<sub>2</sub>.

**FIGURE 6** Schematic diagram of the mechanism for the synthesis of WB<sub>2</sub> powders in the salt melt.

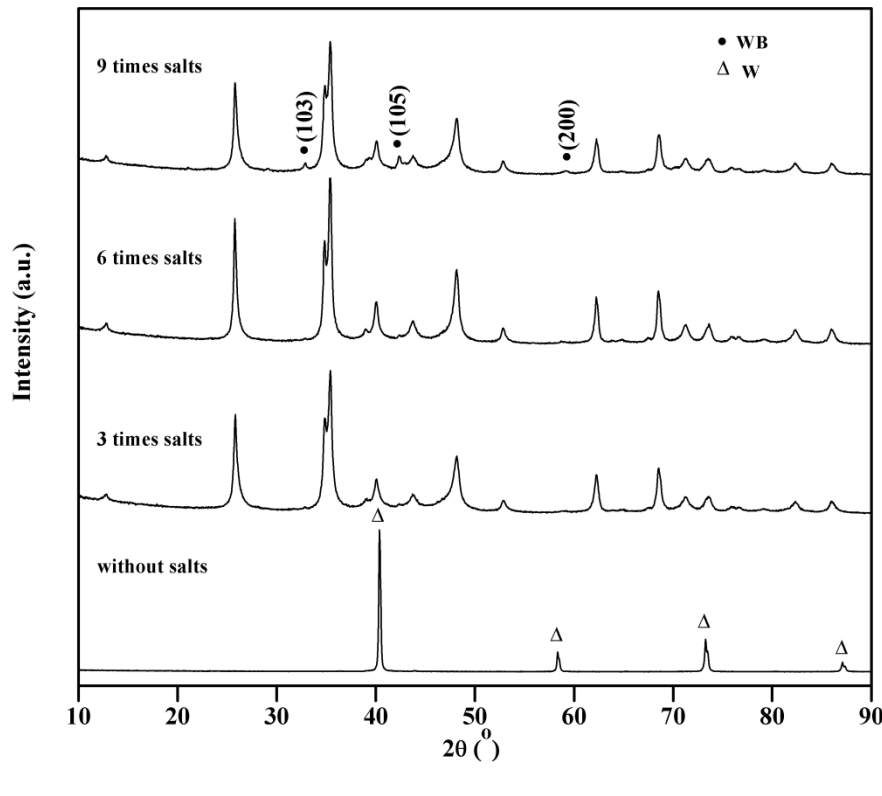
**FIGURE 7** The TG-DSC-DTG curves of the sample in the flowing air at temperatures range 0-1000°C.



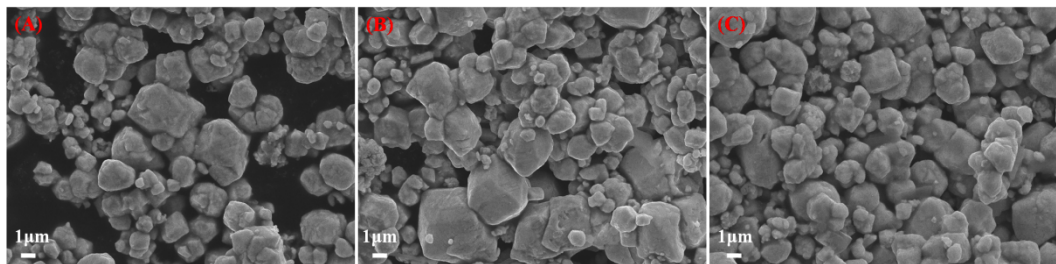
ijac\_13427\_f1.tif



ijac\_13427\_f2.tif

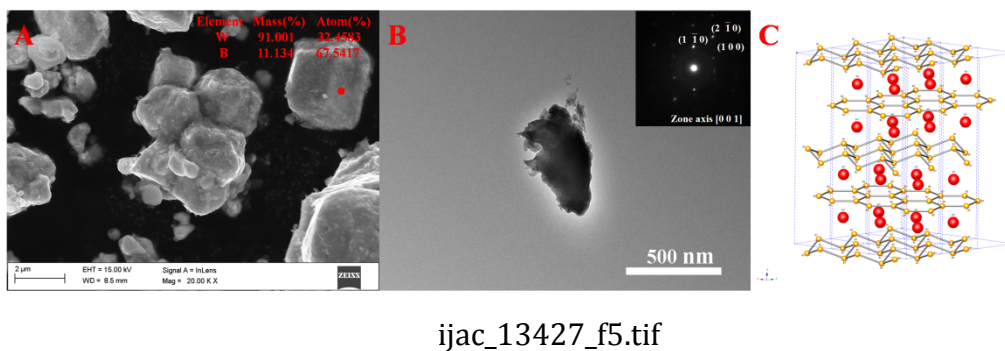


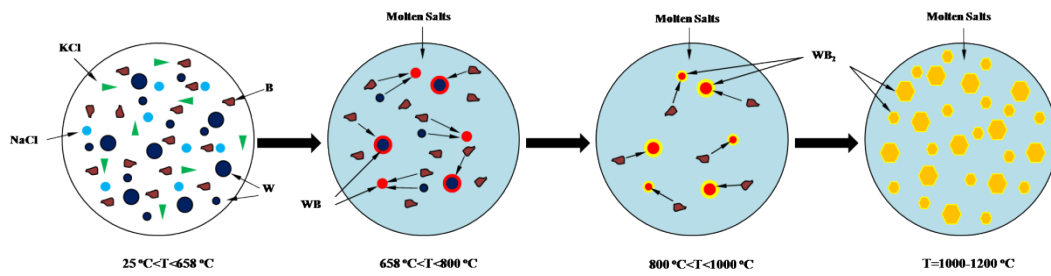
Accepted Article



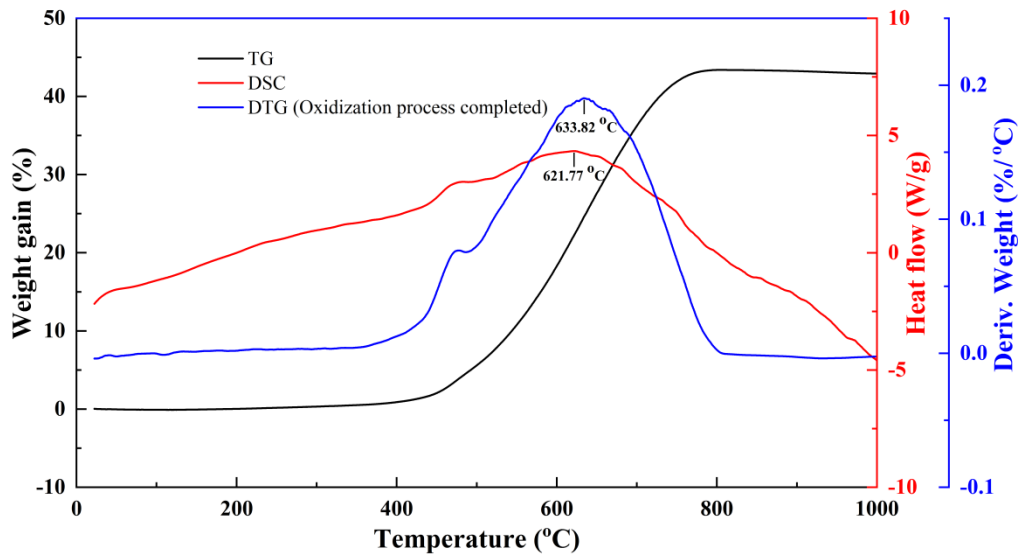
ijac\_13427\_f4.tif

# Accepted Article





ijac\_13427\_f6.tif



ijac\_13427\_f7.tif